Comparison of three seemingly similar lytic polysaccharide monooxygenases from *Neurospora crassa* suggests different roles in plant biomass degradation

Dejan M. Petrović[1], Anikó Várnai[1,*], Maria Dimarogona[2,3], Geir Mathiesen[1], Mats Sandgren[2], Bjørge Westereng[1], and Vincent G.H. Eijsink[1]

From the [1]Faculty of Chemistry, Biotechnology and Food Science, Norwegian University of Life Sciences (NMBU), 1432 Ås, Norway; [2]Department of Molecular Sciences, Swedish University of Agricultural Sciences, 75007 Uppsala, Sweden; [3]Laboratory of Biotechnology and Structural Biology, Department of Chemical Engineering, University of Patras, 26504 Patras, Greece

*To whom correspondence should be addressed: Anikó Várnai: Faculty of Chemistry, Biotechnology and Food Science, Norwegian University of Life Sciences (NMBU), 1432 Ås, Norway; aniko.varnai@nmbu.no; Tel.+47 6723 2569.

SUPPORTING INFORMATION

Supplementary Tables (S1) and Figures (S1-S10)

TABLE S1

Table S1. X-ray data collection and refinement statistics for the structure of *Nc*LPMO9A (catalytic domain)

Data collection	
Space group	$P3_221$
Cell dimensions (a, b, c) (Å)	a=80.4, b=80.4, c=57.9
α, β, γ (°)	90, 90, 120
No. of molecules per asymmetric unit	1
Station (synchrotron)	ID23-2 (ESRF, Grenoble)
Wavelength (Å)	0.8726
Resolution* (Å)	44.51-1.6 (1.63-1.6)
No. of observations	269267
No. of unique reflections	28860
Completeness* (%)	100 (100)
*R*merge[1] (%)	9.8 (100)
Mean((I/sd(I))*	14 (2.3)
CC1/2*	99.9 (69.8)
Multiplicity*	9.3 (8.9)
Refinement	
R_{work}/R_{free} (%)	0.154/0.178
R.m.s.d., bond lengths (Å)	0.009
R.m.s.d., bond angles (°)	1.35
No. of reflections	27351
No. of protein atoms	1632
No. of solvent molecules	243
No. of sulfate ions	3
No. of mannose residues	2
No. of metal atoms	2 (1 Cu, 1 Li)
Average B factor (Å^2) for protein residues	
Overall	17.73
Main chain atoms	17.15
Side chain atoms	18.4
Average B factor (Å^2) for heteroatoms	
Water molecules	30.06
Metal atoms	14.57 (Cu) 24.27 (Li)
Mannose residues	50.93
Sulfate ions	63.97
Ramachandran plot[2] (%)	
Favoured region	98.14
Outliers	0
PDB entry	5FOH

*Highest resolution shell is shown in parentheses

[1] $R_{merge} = \Sigma_{hkl} \Sigma_i | I_i(hkl) - \langle I(hkl) \rangle | / \Sigma_{hkl} \Sigma_i I_i(hkl)$

[2] Calculated using a strict boundary Ramachandran plot

FIGURE S1

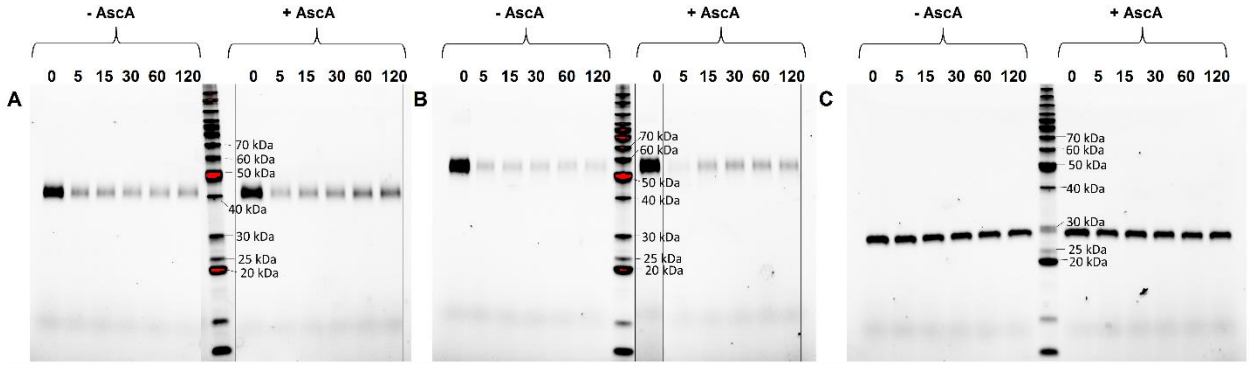

Figure S1. SDS-PAGE of unbound C4 oxidizing *Nc*LPMOs during incubation with 2 mg·ml^{-1} PASC, in the absence (-AscA) or presence (+AscA) of 1 mM ascorbic acid. The amounts of unbound (A) *Nc*LPMO9A, (B) *Nc*LPMO9C, and (C) *Nc*LPMO9D were determined by SDS-PAGE at different time points after starting the incubation of enzyme with substrate. The unbound fractions were separated by filtration through 0.22 µM filter and 2.5 µL of the filtrates were incubated with 2.5 µL of SDS sample buffer and loaded onto the gels.

FIGURE S2

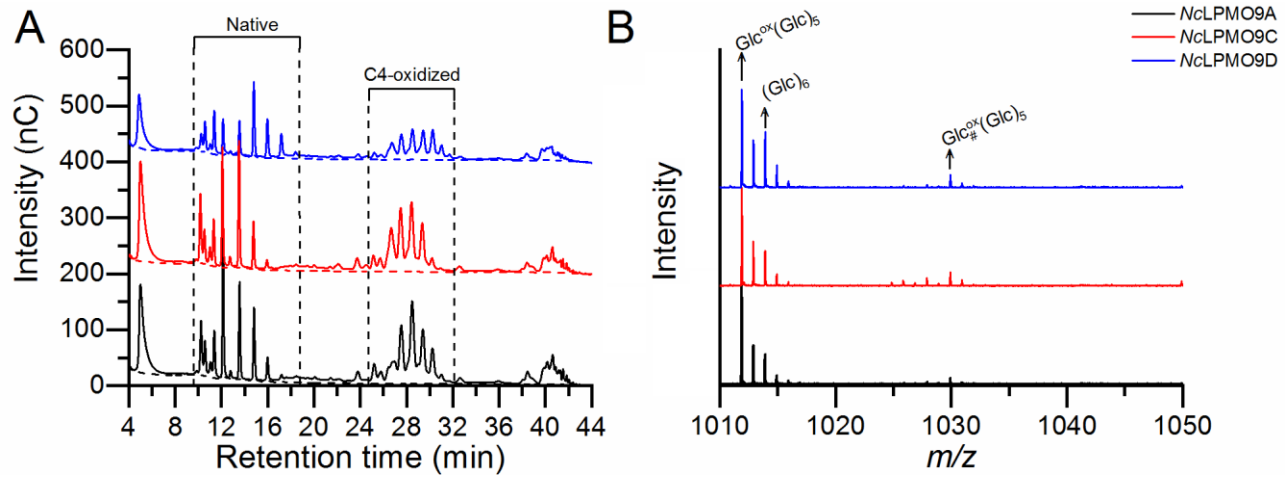

Figure S2. Soluble products generated from PASC by C4 oxidizing *Nc*LPMOs. (A) HPAEC-PAD profiles of reaction mixtures containing *Nc*LPMO9A (black), *Nc*LPMO9C (red) or *Nc*LPMO9D (blue), and PASC, with (solid lines) and without (dashed lines) ascorbic acid. The produced oxidized cello-oligosaccharides are labeled in the figure and annotations are based on previous work (Isaksen, Westereng et al. 2014). (B) Close-up of the DP 6 cluster in a MALDI-ToF MS spectrum of the products, showing the sodium adduct of the native, $(Glc)_6$, the oxidized keto-form, $Glc^{ox}(Glc)_5$, and the oxidized gemdiol form, $Glc_{\#}^{ox}(Glc)_5$.

FIGURE S3

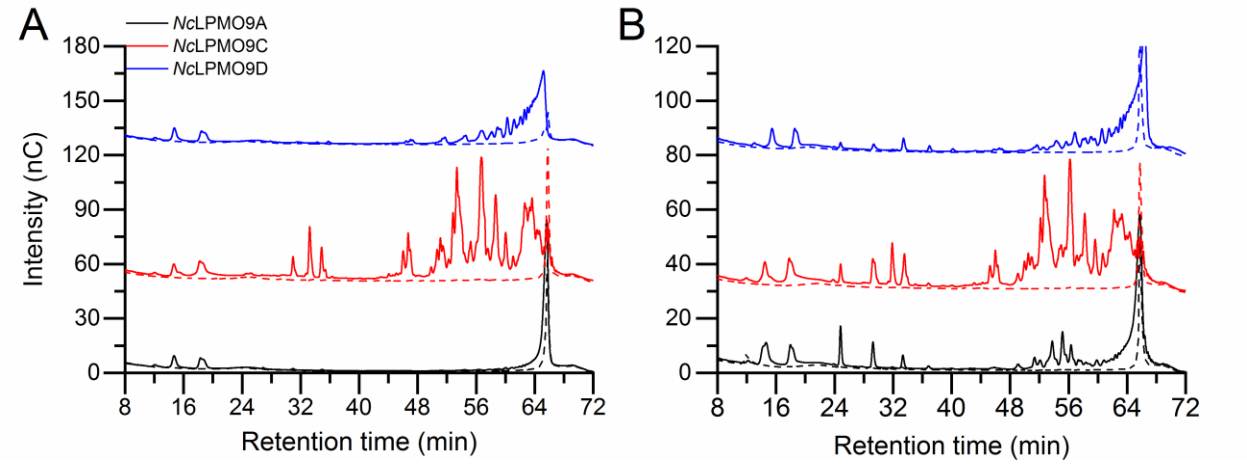

Figure S3. HPAEC-PAD profiles of soluble reaction products generated by C4 oxidizing *Nc*LPMOs from (A) TXG and (B) TXG coated on PASC. Reaction mixtures contained 1 µM NcLPMO9A (black), 1 µM NcLPMO9C (red) or 1 µM NcLPMO9D (blue), and (A) 2 mg·mL^{-1} TXG, or (B) 2 mg·mL^{-1} TXG and 2 mg·mL^{-1} PASC, with (solid lines) and without (dashed lines) ascorbic acid.

FIGURE S4

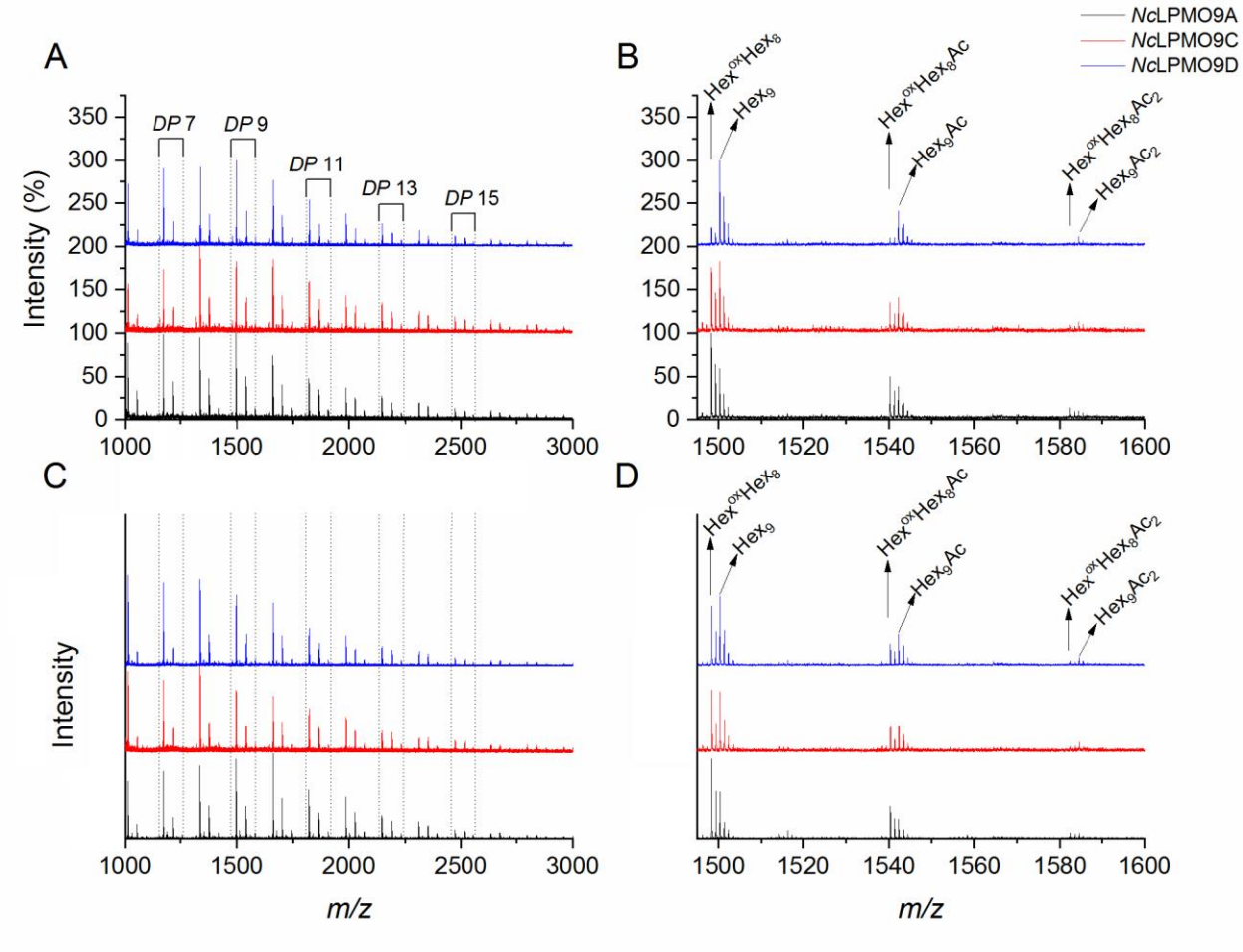

Figure S4. Reaction products generated from konjac glucomannan (KGM), or from KGM coated on PASC. The figures show MALDI-ToF MS spectra of products generated from KGM (A), with a close-up of the *DP* 9 cluster (B), or KGM coated on PASC (C), with a close-up of the *DP* 9 cluster (D), by *Nc*LPMO9A (black), *Nc*LPMO9C (red) and *Nc*LPMO9D (blue). Brackets indicate product clusters of the same *DP*. Due to the identical *m/z* values of KGM and PASC products, it is not possible to distinguish them by MALDI-ToF MS, however, the appearance of acetylated and double acetylated products (typical for KGM), as well as their oxidized forms, confirms activity on KGM (acetylated products were not observed in reactions with only PASC; Fig. S2B). Abbreviations: Hex, hexose (+162 Da); Ac, acetyl group (+42 Da); ox, oxidized (-2 Da for keto form). The species in panels B and D include: native DP9, (*m/z* 1500), oxidized DP9 (-2 Da; *m/z* 1498) for DP9), and their acetylated (+42 Da; *m/z* 1542 and 1540, respectively) and double acetylated (+84 Da; *m/z* 1584 and 1582, respectively) forms.

FIGURE S5

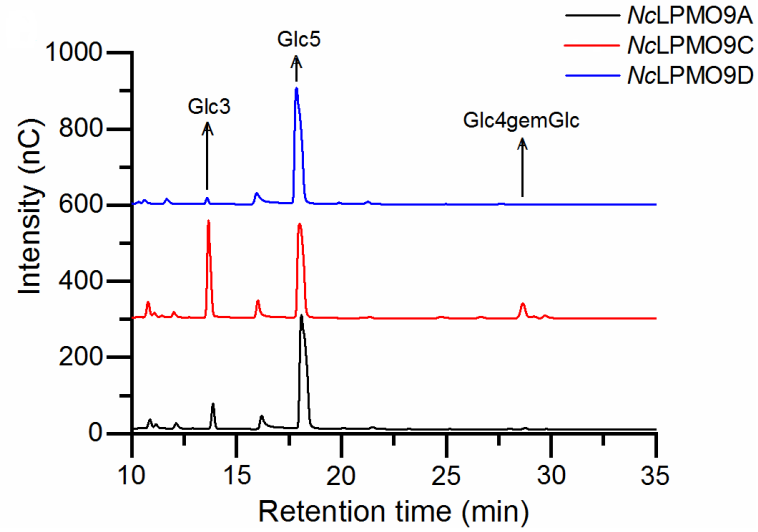

Figure S5. Reaction products generated by C4 oxidizing *Nc*LPMOs from cellopentaose. HPAEC-PAD chromatograms of products generated in reactions containing 1 µM *Nc*LPMO9A (black line), 1 µM *Nc*LPMO9C (red line) or 1 µM *Nc*LPMO9D (blue line), and 2.4 mM cellopentaose in the presence of 1 mM ascorbic acid (the oxidized product, Glc_4gemGlc, is labeled). In control reactions without ascorbic acid, the cellopentaose was not cleaved.

FIGURE S6

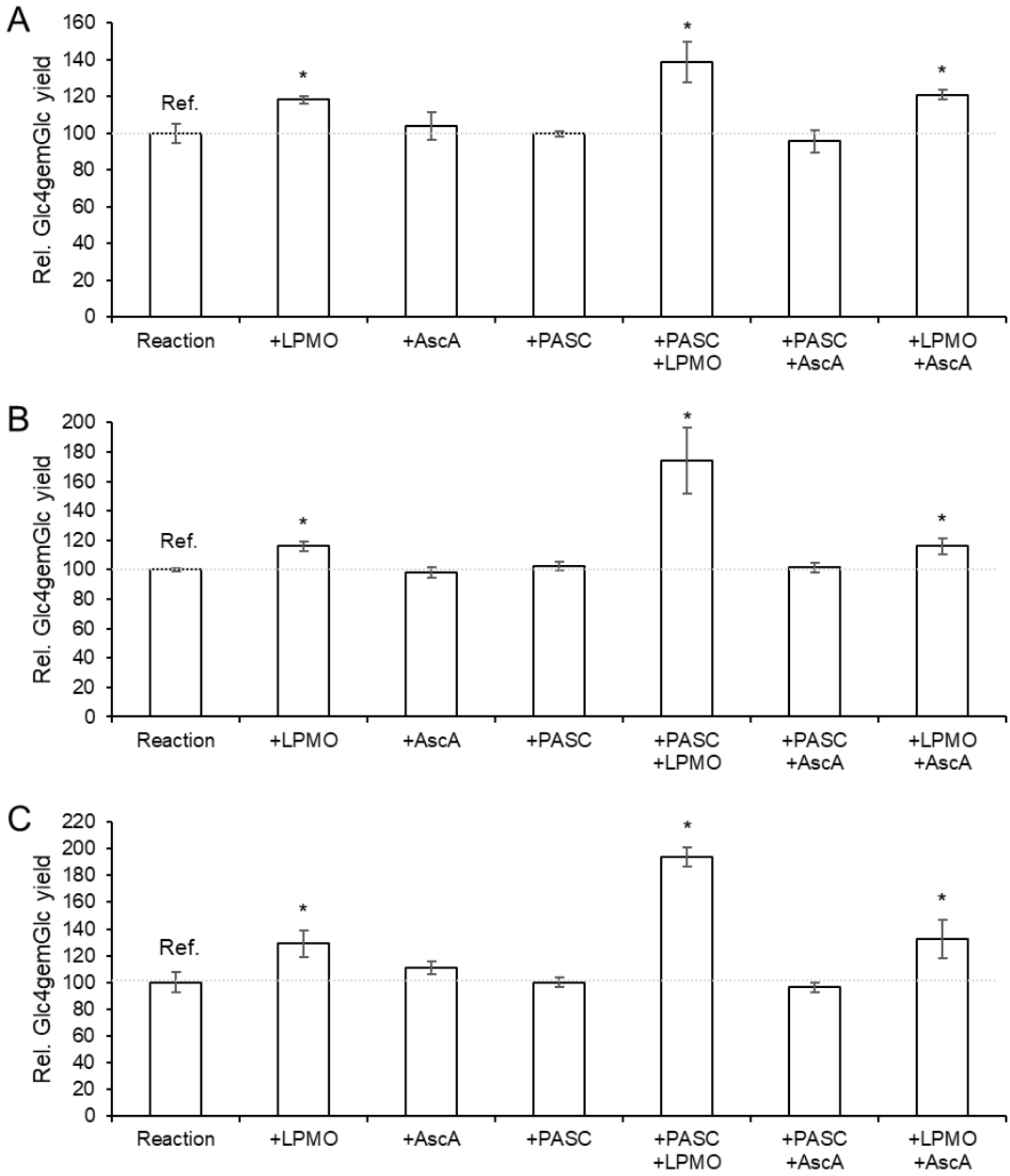

Figure S6. Control experiments to assess the cause of the arrest in product formation by LPMOs. Reactions were set up as in Figure 6C: 2 mg·ml^{-1} PASC was incubated with 1 µM (A) *Nc*LPMO9A, (B) *Nc*LPMO9C or (C) *Nc*LPMO9D and 3.3 mM AscA in 50 mM Bis-Tris, pH 6.5, at 45 °C and 1000 rpm. After 240 min incubation (i.e., the end point in Fig. 6C), 100 µl of the reaction mixtures were supplemented with 50 µl buffer or buffer containing various combinations of PASC, LPMO and AscA, followed by incubation for another 120 min. Solubilized oxidized products were enzymatically converted to Glc4gemGlc using 1 µM *Tr*Cel7A, and the concentrations of Glc4gemGlc were determined by HPAEC-PAD, as in Figure 6. Samples were run in triplicates; error bars represent standard deviations. Product levels with statistically significant (one-tailed Student's t-test at α=0.05 significance level, probability $p<0.05$) differences from the reference ("Buffer") are marked with an asterisk. Note that additional Glc4gemGlc was only produced when the reaction mixture was supplemented with LPMO; addition of PASC, AscA or both, in the absence of added LPMO, did not have a significant effect on the Glc4gemGlc yield.

FIGURE S7

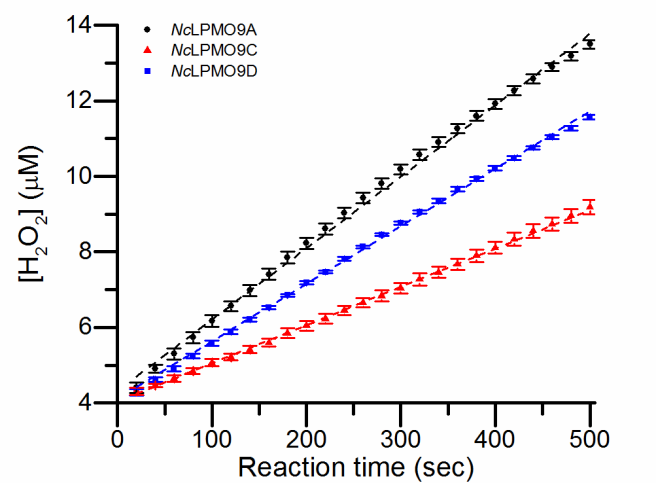

Figure S7. Generation of H_2O_2 by C4 oxidizing *Nc*LPMOs. 1 μM of *Nc*LPMO9A (black), *Nc*LPMO9C (red) or *Nc*LPMO9D (blue) were incubated with 50 μM ascorbic acid in the absence of substrate, and the apparent production of H_2O_2 was measured as described in "Materials and methods". The figure shows data points in the linear region of the progress curves and error bars indicate standard deviations calculated from three experiments.

FIGURE S8

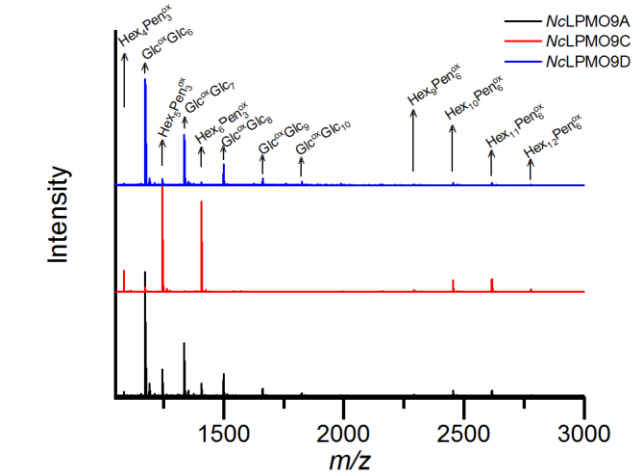

Figure S8. Reaction products generated by C4 oxidizing *Nc*LPMOs from TXG coated on PASC with H_2O_2 as a co-substrate. MALDI-ToF MS spectra showing product profiles generated from a mixture of 2 mg·mL^{-1} TXG and 2 mg·mL^{-1} PASC by 1 µM *Nc*LPMO9A (black), *Nc*LPMO9C (red) or *Nc*LPMO9D (blue) in 50 mM Bis-Tris, pH 6.5, at 45 °C and 1000 rpm, with addition of ~45 µM H_2O_2 to the reactions every 15 min for 4 h. Prior to every addition of H_2O_2, ~12 µM of ascorbic acid was added to ensure reduction of the LPMO. Control reactions were done in the absence of H_2O_2 meaning that only ~12 µM ascorbic acid was added every 15 min for 4 h. In the control reactions only minute amounts of the oxidized products were detected. Oxidized products characteristic for xyloglucan ($Hex_4Pen_3^{ox}$; $Hex_5Pen_3^{ox}$; $Hex_6Pen_3^{ox}$; $Hex_9Pen_6^{ox}$; $Hex_{10}Pen_6^{ox}$; $Hex_{11}Pen_6^{ox}$; and $Hex_{12}Pen_6^{ox}$) and for cellulose ($Glc^{ox}(Glc)_6$; $Glc^{ox}(Glc)_7$; $Glc^{ox}(Glc)_8$; $Glc^{ox}(Glc)_9$; and $Glc^{ox}(Glc)_{10}$), were identified. Abbreviations: Hex, hexose (+162 Da); Pen, pentose (+132 Da); Glc, glucose; ox, oxidized. For more discussion of the structure of the products, see the legend of Fig. 4 in the main manuscript.

FIGURE S9

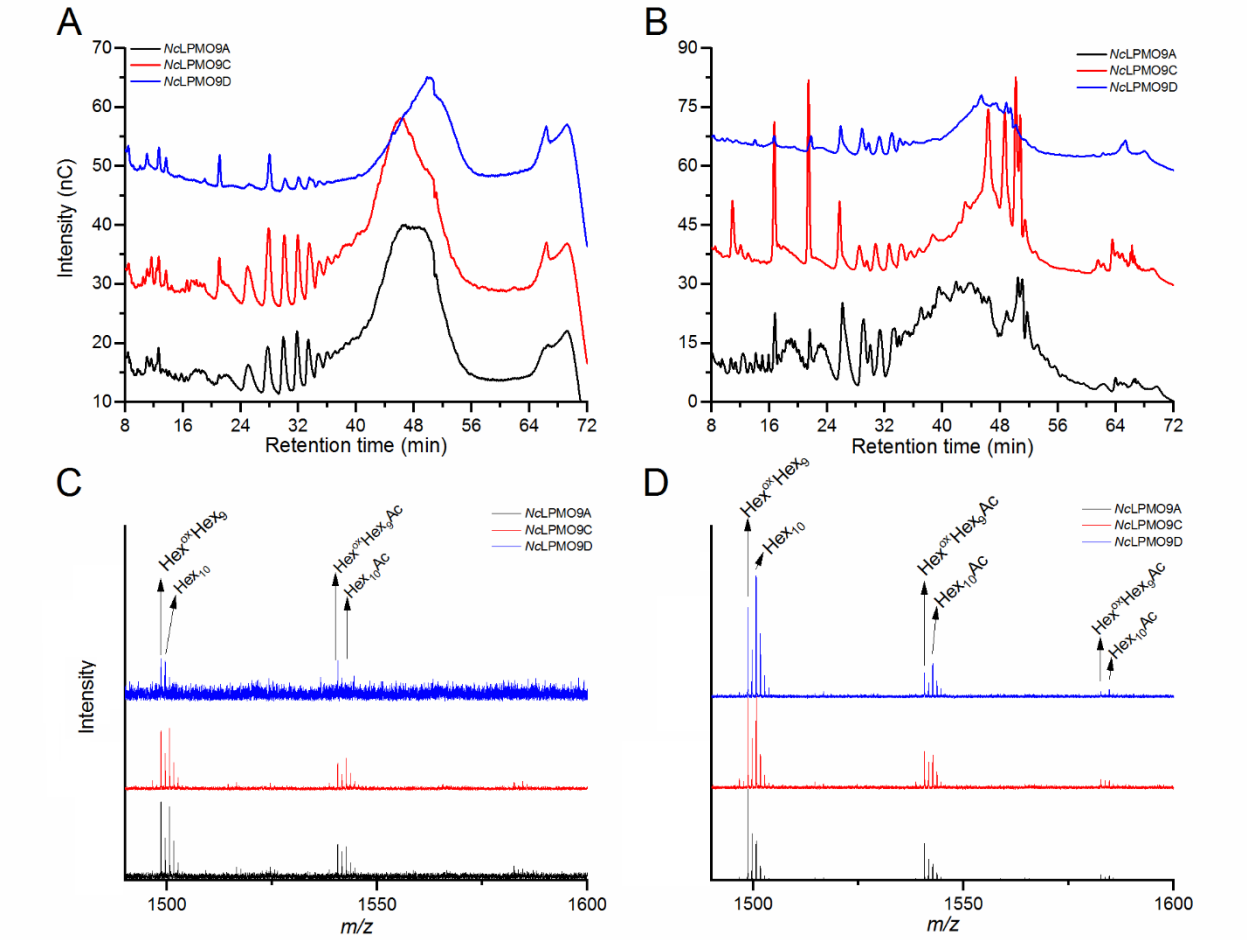

Figure S9. Reaction products generated by C4 oxidizing *Nc*LPMOs from KGM or KGM coated on PASC with H_2O_2 as a co-substrate. Reaction mixtures contained 1 µM *Nc*LPMO9A (black), 1 µM *Nc*LPMO9C (red) or 1 µM *Nc*LPMO9D (blue), and 2 mg·mL^{-1} KGM, or 2 mg·mL^{-1} KGM and 2 mg·mL^{-1} PASC. (A) HPAEC-PAD profiles of soluble reaction products generated from 2 mg·mL^{-1} KGM by 1 µM *Nc*LPMO9A (black), 1 µM *Nc*LPMO9C (red) or 1 µM *Nc*LPMO9D (blue), in 50 mM Bis-Tris, pH 6.5, at 45 °C and 1000 rpm, with addition of ~45 µM H_2O_2 to the reactions every 15 min for 4 h. Prior to every addition of H_2O_2, ~12 µM of ascorbic acid was added to ensure reduction of the LPMO. Products appear in the HPAEC-PAD chromatograms in the range between 24 and 40 min. (B) HPAEC-PAD profiles of soluble reaction products generated from a mixture of 2 mg·mL^{-1} KGM and 2 mg·mL^{-1} PASC by 1 µM *Nc*LPMO9A (black), 1 µM *Nc*LPMO9C (red) or 1 µM *Nc*LPMO9D (blue), in 50 mM Bis-Tris, pH 6.5, at 45 °C and 1000 rpm, using the same feeding of H_2O_2 and ascorbic acid as in panel A. Sharp peaks appearing at 11, 16, 21 and 25 min (absent in the reactions with only KGM) are cello-oligomers; peaks reflecting C4-oxidized cello-oligomers are not clearly visible because they overlap with peaks of KGM-derived products. (C) MALDI–ToF MS of soluble reaction products generated from KGM, showing a close up of the DP9 cluster. (D) MALDI–ToF MS of soluble reaction products generated from KGM coated on PASC, showing a close up of the DP9 cluster. Abbreviations: Hex, hexose (+162 Da); Ac, acetyl group (+42 Da); ox, oxidized (-2 Da for keto form). Control reactions without addition of H_2O_2, i.e. addition of ascorbic acid only, showed minute amounts of products, due to LPMO reactions fueled by ascorbic acid, at very low concentration, and O_2 (not shown).

FIGURE S10

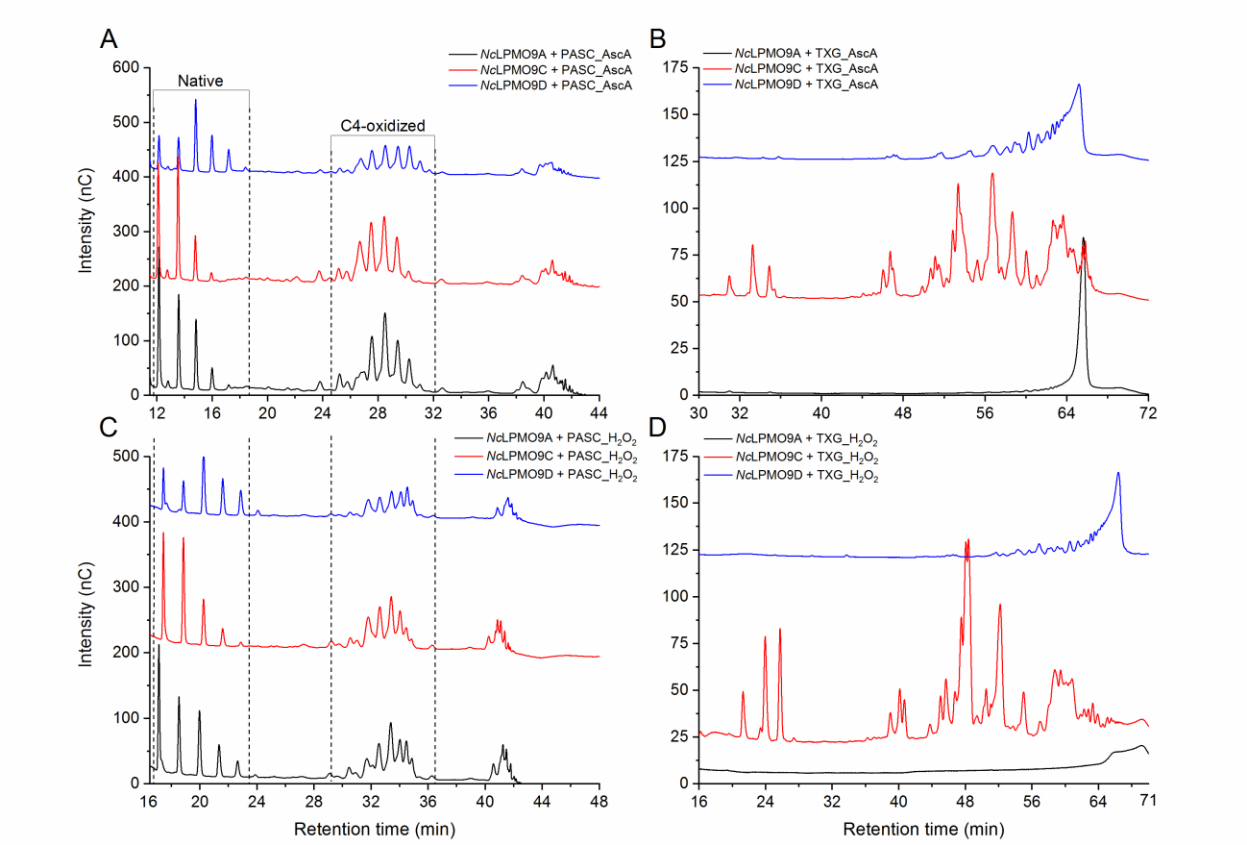

Figure S10. Comparison of the soluble products generated by C4 oxidizing *Nc*LPMOs from PASC or TXG in reactions with only O_2 or with H_2O_2. This figure is a compilation of Figures 7A, 7B, S2A and S3A showing similarities between the product profiles generated in reactions with O_2 and mM amounts of ascorbic acid (A, B) or with H_2O_2 and priming amounts of ascorbic acid (C, D)**.** Due to considerable drift in the chromatographic system, retention times vary, but the similarities in the peak profiles are nevertheless clear. (A and C) HPAEC-PAD profiles of soluble products generated by 1 µM *Nc*LPMO9A (black line), 1 µM *Nc*LPMO9C (red line) or 1 µM *Nc*LPMO9D (blue line), in reactions with 2 mg·mL^{-1} PASC and (A) 1 mM ascorbic acid or (C) addition of ~45 µM H_2O_2 to the reactions every 15 min for 4 h (prior to every addition of H_2O_2, ~12 µM of ascorbic acid was added to ensure reduction of the LPMO), in 50 mM Bis-Tris, pH 6.5, at 45 °C and 1000 rpm. Dashed lines indicate the elution regions of native and oxidized cello-oligomers. (B and D) HPAEC-PAD profiles of soluble products generated by 1 µM *Nc*LPMO9A (black line), 1 µM *Nc*LPMO9C (red line) or 1 µM *Nc*LPMO9D (blue line), in reactions with 2 mg·mL^{-1} TXG and (B) 1 mM ascorbic acid or (D) addition of ~45 µM H_2O_2 to the reactions every 15 min for 4 h (prior to every addition of H_2O_2, ~12 µM of ascorbic acid was added to ensure reduction of the LPMO), in 50 mM Bis-Tris, pH 6.5, at 45 °C and 1000 rpm.